



HAL
open science

Myocardial fibrosis assessed by magnetic resonance imaging in asymptomatic heterozygous familial hypercholesterolemia: the cholcoeur study

Antonio Gallo, Philippe Giral, David Rosenbaum, Alessandro Mattina, Ali Kilinc, Alain Giron, Khaoula Bouazizi, Moussa Gueda Moussa, Joe-Elie Salem, Alain Carrié, et al.

► To cite this version:

Antonio Gallo, Philippe Giral, David Rosenbaum, Alessandro Mattina, Ali Kilinc, et al.. Myocardial fibrosis assessed by magnetic resonance imaging in asymptomatic heterozygous familial hypercholesterolemia: the cholcoeur study. *EBioMedicine*, 2021, 74, pp.103735. 10.1016/j.ebiom.2021.103735 . hal-03468656

HAL Id: hal-03468656

<https://hal.sorbonne-universite.fr/hal-03468656v1>

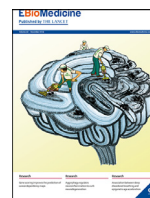
Submitted on 7 Dec 2021

HAL is a multi-disciplinary open access archive for the deposit and dissemination of scientific research documents, whether they are published or not. The documents may come from teaching and research institutions in France or abroad, or from public or private research centers.

L'archive ouverte pluridisciplinaire **HAL**, est destinée au dépôt et à la diffusion de documents scientifiques de niveau recherche, publiés ou non, émanant des établissements d'enseignement et de recherche français ou étrangers, des laboratoires publics ou privés.



Distributed under a Creative Commons Attribution 4.0 International License



Myocardial fibrosis assessed by magnetic resonance imaging in asymptomatic heterozygous familial hypercholesterolemia: the cholcoeur study

Antonio Gallo^{a,b,c,d,*}, Philippe Giral^a, David Rosenbaum^a, Alessandro Mattina^{a,e}, Ali Kilinc^c, Alain Giron^b, Khaoula Bouazizi^c, Moussa Gueda Moussa^b, Joe-Elie Salem^{f,g}, Alain Carrié^h, Valérie Carreau^a, Sophie Béliard^{i,j}, Randa Bittar^k, Philippe Cluzel^l, Eric Bruckert^{a,c}, Alban Redheuil^{b,c,l}, Nadja Kachenoura^{b,c}

^a Cardiovascular Prevention Unit, Department of Endocrinology, Metabolism and cardiovascular prevention—University Hospital Pitié-Salpêtrière – Assistance Publique/Hôpitaux de Paris, Groupe Hospitalier Pitié-Salpêtrière – Sorbonne University

^b Sorbonne University, Biomedical Imaging Laboratory, CNRS, INSERM, Paris, France

^c Sorbonne University, INSERM, Institute of Cardio-metabolism and Nutrition (ICAN), Imaging Core Lab, Hôpital de la Pitié-Salpêtrière, Paris, France

^d Université de La Réunion, INSERM, UMR 1188 Diabète athéromatose, Réunion Océan Indien (DéTROI), Saint-Denis de La Réunion, France

^e Diabetes and Islet Transplantation Unit, Department of Diagnostic and Therapeutic Services, IRCCS-ISMETT (Istituto Mediterraneo per i Trapianti e Terapie ad alta specializzazione), University of Pittsburgh Medical Center - Italy, Palermo, Italy

^f AP-HP, Pitié-Salpêtrière Hospital, Department of Pharmacology and CIC-1901, F-75013 Paris, France

^g INSERM, CIC-1901 and UMR 1166, F-75013 Paris, France, Sorbonne Universités

^h Sorbonne University, Inserm, UMR_S1166, APHP, Department of Biochemistry, Obesity and Dyslipidemia Genetics Unit, Hôpital de la Pitié, Paris, France

ⁱ Aix Marseille Univ, INSERM, INRA, C2VN, Marseille, France

^j Department of Nutrition, Metabolic Diseases, Endocrinology, La Conception Hospital, Marseille, France

^k Sorbonne University, Inserm, UMR_S1166, Department of Metabolic Biochemistry, Assistance Publique, Hôpitaux de Paris, Hôpital de la Pitié-Salpêtrière, Paris, France

^l Cardiovascular and Thoracic Imaging Unit, Assistance Publique-Hôpitaux de Paris, Groupe Hospitalier Pitié-Salpêtrière, Sorbonne University, INSERM, Paris, France

ARTICLE INFO

Article History:

Received 27 September 2021

Revised 15 November 2021

Accepted 19 November 2021

Available online xxx

Keywords:

Familial hypercholesterolemia
cardiovascular imaging
cardiac magnetic resonance
primary prevention
genetic dyslipidaemia
cardiovascular risk

ABSTRACT

Background: Familial Hypercholesterolemia (FH) is an underdiagnosed condition with an increased cardiovascular risk. It is unknown whether lipid accumulation plays a role in structural myocardial changes. Cardiovascular Magnetic Resonance (CMR) is the reference technique for the morpho-functional evaluation of heart chambers through cine sequences and for myocardial tissue characterization through late gadolinium enhancement (LGE) and T1 mapping images. We aimed to assess the prevalence of myocardial fibrosis in FH patients.

Methods: Seventy-two asymptomatic subjects with genetically confirmed FH (mean age 49.24, range 40 to 60 years) were prospectively recruited along with 31 controls without dyslipidaemia matched for age, sex, BMI, and other cardiovascular risk factors. All underwent CMR including cine, LGE, pre- and post-contrast T1 mapping. Extracellular volume (ECV) and enhancement rate of the myocardium (ERM = difference between pre- and post-contrast myocardial T1, normalized by pre-contrast myocardial T1) were calculated.

Findings: Five FH patients and none of the controls had intramyocardial LGE ($p=0.188$). While no changes in Native T1 and ECV were found, post-contrast T1 was significantly lower ($430.6 \pm 55\text{ms}$ vs. $476.1 \pm 43\text{ms}$, $p<0.001$) and ERM was higher ($57.44 \pm 5.99\%$ vs 53.04 ± 4.88 , $p=0.005$) in HeFH patients compared to controls. Moreover, low post-contrast T1 was independently associated with the presence of xanthoma (HR 5.221 [1.04-26.28], $p=0.045$). A composite score combining the presence of LGE, high native T1 and high ERM (defined as \geq mean ± 1.5 SD) was found in 20.8% of the HeFH patients vs. 0% in controls ($p<0.000$, after adjustment for main confounders).

* Corresponding author: Antonio Gallo, MD PhD, Université de La Réunion, INSERM, UMR 1188 Diabète athéromatose, Réunion Océan Indien (DéTROI), Laboratoire CYROI, 2 Rue Maxime Rivière, 97490 Saint-Denis de La Réunion, France
E-mail address: antoniogallo.md@gmail.com (A. Gallo).

Interpretation: CMR revealed early changes in myocardial tissue characteristics in HeFH patients, that should foster further work to better understand and prevent the underlying pathophysiological processes.

© 2021 The Authors. Published by Elsevier B.V. This is an open access article under the CC BY-NC-ND license (<http://creativecommons.org/licenses/by-nc-nd/4.0/>)

Research in Context

Evidence before this study

Heterozygous Familial hypercholesterolemia (HeFH) is a common inherited disease associated with increased cardiovascular risk. A significant variability in the clinical presentation makes it difficult to early detect more severe forms that might need earlier and more aggressive treatment. The management of this condition is evolving due to novel diagnostic and therapeutic development. Investigations through computed tomography for coronary artery calcium and echocardiography for diastolic function have shown that hypercholesterolemic subjects have an early impairment of the vascular tree and an earlier myocardial dysfunction. To date, no investigations have been performed to characterize myocardial tissue changes in familial hypercholesterolemia. Cardiac magnetic resonance is an optimal tool for the functional and morphological analysis of myocardium.

Added value of this study

In this study we found a decreased post-contrast T1 in asymptomatic HeFH patients, compared to non-hypercholesterolemic controls, pointing an expansion of the interstitial space that suggests interstitial fibrosis. The presence of xanthoma at diagnosis, suggesting a more severe clinical presentation of HeFH, was independently associated with a lower myocardial post-contrast T1. Our results suggest that on top of coronary atherosclerosis, a lipidic infiltration takes place in the myocardium of hypercholesterolemic subjects.

Implications of all the available evidence

The results of this study challenge clinicians on the possibility of a parallel non-atherosclerotic physiopathological pattern in HeFH, raising the question on the prevention of heart failure in stabilized on-target HeFH subjects. Further translational research is needed to better elucidate the physiopathological process underlying myocardial lipid accumulation and correlate imaging findings with molecular processes taking place in this genetic disease.

1. Introduction

Heterozygous familial hypercholesterolemia (HeFH) is a common genetic disease associated with a high risk of coronary heart disease (CHD) due to lifelong exposure to high LDL-cholesterol (LDL-C) levels [1,2]. Big efforts are being made in order to improve clinical recognition, increase awareness, and develop alternative strategies for a more efficient therapeutic management of HeFH patients [3]. Although several studies have shown an increased prevalence of sub-clinical atherosclerotic cardiovascular disease (ASCVD) [4,5] in HeFH, there is still no consensus regarding the clinical value of cardiovascular imaging in asymptomatic HeFH patients.

Despite being considered a high cardiovascular risk condition, HeFH is also associated with an extreme phenotypic variability, which leads to an overall underestimation of the disease prevalence

and pathogenicity [6]. While coronary arteries represent the prime territory for disease in HeFH, other risk factors may involve other cardiovascular territories. An increase in LDL-C levels has been associated with impaired microvascular function, which can ultimately lead to myocardial tissue impairment [7].

Cardiac Magnetic Resonance (CMR) is the reference technique for the evaluation of cardiac morphology, systolic function as well as the detection and quantification of myocardial scar on late gadolinium enhancement (LGE) images. CMR mapping sequences have recently emerged for non-invasive myocardial interstitial fibrosis and oedema characterization in several cardiomyopathies [8–10].

If coronary arteries and aortic valves have been widely studied in HeFH patients, [11,12] studies on myocardial tissue characterization in this population are lacking. We accordingly designed the present study to 1) investigate myocardial tissue by CMR in patients with a genetic diagnosis of HeFH free of ASCVD and estimate the prevalence of myocardial fibrosis, 2) investigate concurrent systolic cardiac function, and 3) determine how CMR biomarkers relate to markers of increased lifelong exposure to high cholesterol levels.

2. Methods

2.1. Study population and design

The Cholcoeur Study (Clinical Trial N° NCT02517944) is an observational prospective case-control monocentric study.

One-hundred and three subjects (60 men, 43 women) aged between 40 and 60 years (mean age 49.24±4.66) were consecutively enrolled between October 2014 and June 2017 at the Cardiovascular Prevention Unit of Pitié-Salpêtrière Hospital in Paris, France according to the following inclusion criteria: genetically confirmed HeFH, no symptoms or electrocardiographic signs of ischemia, no personal history of CHD. Exclusion criteria were the absence of health insurance, refusal after informed consent, contra-indication to CMR, pregnancy, diabetes mellitus, uncontrolled hypertension.

Control subjects were matched for age, body mass index (BMI), smoking habits. They were consecutively enrolled at the Centre for Clinical Investigation (Centre d'Investigation Clinique, CIC) at Pitié-Salpêtrière Hospital in Paris, France.

Arterial hypertension was defined as office Systolic BP (SBP) ≥140 mmHg and/or Diastolic BP (DBP) ≥90 mmHg and/or use of antihypertensive medication. Diabetes mellitus was defined as Fasting Plasma Glucose (FPG) levels ≥7.0 mmol/L or HbA_{1c}>6.5% and/or antidiabetic treatment. Current smoking was defined as having smoked at least one cigarette in the last 30 days. Glomerular filtration rate (GFR) was assessed according to the Modification of Diet for Renal Disease study equation. Patients' anthropometric characteristics such as BMI and body surface area (BSA) were also calculated.

High intensity statin dose was defined as previously described (atorvastatin 40 or 80 mg/day, rosuvastatin 20 or 40 mg/day, or simvastatin 80 mg/day) [13].

Both HeFH patients and controls underwent a CMR exam on the same day as clinical and biological tests were performed for this study.

2.2. CMR imaging and analysis

All subjects underwent a CMR exam on a 1.5T magnet (Magnetom Aera, Siemens Healthineers, Erlangen, Germany) using a thoracic

phased array coil including the following sequences: 1) cine short and long axis slices covering the left ventricle and atrium using steady state free precession (SSFP), 2) short and long axis LGE T1-weighted single shot inversion recovery images were acquired 10 minutes after IV injection of 0.2 mmol/kg of Gd-DTPA (Dotarem®, Guerbet, France) with inversion time chosen to null the normal myocardium, 3) motion-corrected basal, and mid-LV short-axis modified look-locker inversion-recovery (MOLLI) T1 mapping sequence before and 15 minutes after contrast injection, 4) motion-corrected basal and mid-LV short-axis T2 mapping using a 3-point T2-prepared SSFP sequence performed before contrast injection.

CMR data were analysed using QMass v.6 (Medis, the Netherlands) by the same operator blinded to study groups and to clinical data. Left ventricular (LV) end-diastolic and end-systolic volumes as well as LV mass were measured after semi-automated tracing of myocardial contours on all contiguous cine SSFP short axis slices. LV ejection fraction, stroke volume and mass-to-volume ratio were appropriately calculated. Similarly, right ventricular (RV) end-diastolic and end-systolic volumes, ejection fraction as well as stroke volume were measured. The same cine images were analysed to visually assess regional LV myocardial function as normokinetic, hypokinetic, akinetic or dyskinetic reported according to the standardized American Heart Association segmentation [14]. Left ventricle longitudinal global strain and strain rate were calculated as the average of 4 and 2 chambers view using CMR feature-tracking, as previously described [15].

Myocardial tissue characterization comprised visual analysis for the presence or absence of LGE, which was performed by an expert reader (more than 15 years of experience). The QMass segmentation tool was used on pre- and post-contrast T1 as well as T2 maps to delineate the LV myocardium and estimate global myocardial T1 and T2 as the average of basal and mid-LV slices. Pre- and post-contrast T1 values in the blood pool were also calculated by carefully positioning a ROI within the LV cavity while avoiding papillary muscles. Myocardial and blood pool T1 measures were subsequently used for the estimation of the partition coefficient (λ) calculated using a previously described formula: $\lambda = (\text{post-contrast } R1_{\text{myo}} - \text{pre-contrast } R1_{\text{myo}}) / (\text{post-contrast } R1_{\text{LV-cavity}} - \text{pre-contrast } R1_{\text{LV-cavity}})$, with $R1 = 1/T1$. Then, the extracellular volume (ECV, %) was calculated as: $(1 - \text{hematocrit}) * \lambda$. Finally, relative myocardial T1 shortening (ERM) was calculated using the following formula: $(\text{pre-contrast } T1_{\text{myo}} - \text{post-contrast } T1_{\text{myo}}) / \text{pre-contrast } T1_{\text{myo}}$. Such index was successfully used to characterize tissue interstitial changes in the liver^{15,16} as well as in the myocardium [18].

2.3. Total cholesterol burden (TCB) calculation

Lifelong cholesterol exposure was estimated by calculating TCB (mg/dL-year) as previously reported [4]. TCB was obtained by multiplying the initial serum total cholesterol (TC) value by the age of the patient at diagnosis onset and by adding the TC values measured annually during follow-up visits. If lipid profiles were missing for more than 50 % of time points TCB was not calculated. Fifty-six FH patients had TCB calculation available for the final analysis.

2.4. Coronary atherosclerotic burden

Each patient underwent a multi-detector CT scan (Definition Flash, Siemens, Erlangen, Germany) for a total radiation exposure of 1 to 3mSv. Coronary artery calcium (CAC) score was calculated according to Agatston method [19]. The detailed procedure of images acquisition and treatment has been previously reported [4]. All CT scans were quantified in an expert central reading centre and supervised by a senior cardiovascular radiologist (AR) who was blinded to patients recent and past medical history.

2.5. Genetic and biochemical testing

Genetic analysis was performed by the Genetic Centre, Pitié-Salpêtrière University Hospital, Paris, France (www.cgmc-psl.fr) while lipid testing was performed at the Lipid Laboratory of the Biochemical Functional Unit at the same institution. Methodology for both testing has been previously described [20].

2.6. Statistics

Statistical analysis was performed by STACTIS, Paris, France. Data represent mean \pm SD for continuous variables, and frequency (percentage) for categorical variables. The difference between the patient and control groups for a continuous variable was tested using Student's t-test or Welch's t-test, when a preliminary F-test rejected the assumption of the equal variances in the 2 normal distributions; or Wilcoxon-Mann-Whitney test, when the 2 previous Shapiro-Wilk tests rejected the assumption of normality. The difference between the 2 groups for a categorical variable was tested using: Pearson's chi-squared test; or, when ≥ 1 expected value was ≤ 5 , Fisher's exact test, with its Freeman-Halton extension for more than two-rows.

The relationship between 2 continuous variables within a group was assessed and tested using both Pearson's product-moment correlation coefficient r ; and Spearman's rank correlation coefficient ρ , in case of ≥ 1 rejected assumption of normality using 2 previous Shapiro-Wilk tests. The relationship between a continuous variable and a dependent dichotomous variable within a group was assessed and tested using: 1) point-biserial correlation coefficient r_{pb} , with the Glass-Hopkins's correction, after verifying for each category of the dichotomous variable that the continuous variable had no significant outliers using quartiles, was approximately normally distributed using the Shapiro-Wilk test, and had equal variances using the Levene's test; 2) binomial logistic regression, after checking the linearity assumption between the continuous variable and the logit transformation of the dichotomous variable using the Box-Tidwell procedure. All tests were 2-sided. A p -value ≤ 0.05 was considered statistically significant.

2.7. Sample size estimation

Statistical power calculation was based on the prevalence of LGE in other asymptomatic cohorts from the literature [21,22]. A sample of 110 subjects (75 HeFH, 35 non-HeFH controls) was considered sufficient to detect a 14.5 points difference (15% vs. 0.5%) in percentage of silent myocardial infarction with a statistical power of 81.7%. The final analysis was performed on 72 HeFH patients and 31 controls: the reason for HeFH patients and controls exclusion is detailed in Figure 1.

3. Ethics statement

The local institutional review board approved the study (N° 2014-A0130641) and written informed consent was received from participants prior to inclusion in the study.

4. Role of Funders

The study was supported by a grant from Amgen, which was not involved in the design and conduct of the study, data analysis and interpretation, or the writing of the manuscript. The ICAN Institute of Cardiometabolism and Nutrition, an Academic hospital organization was responsible for the study conduct.

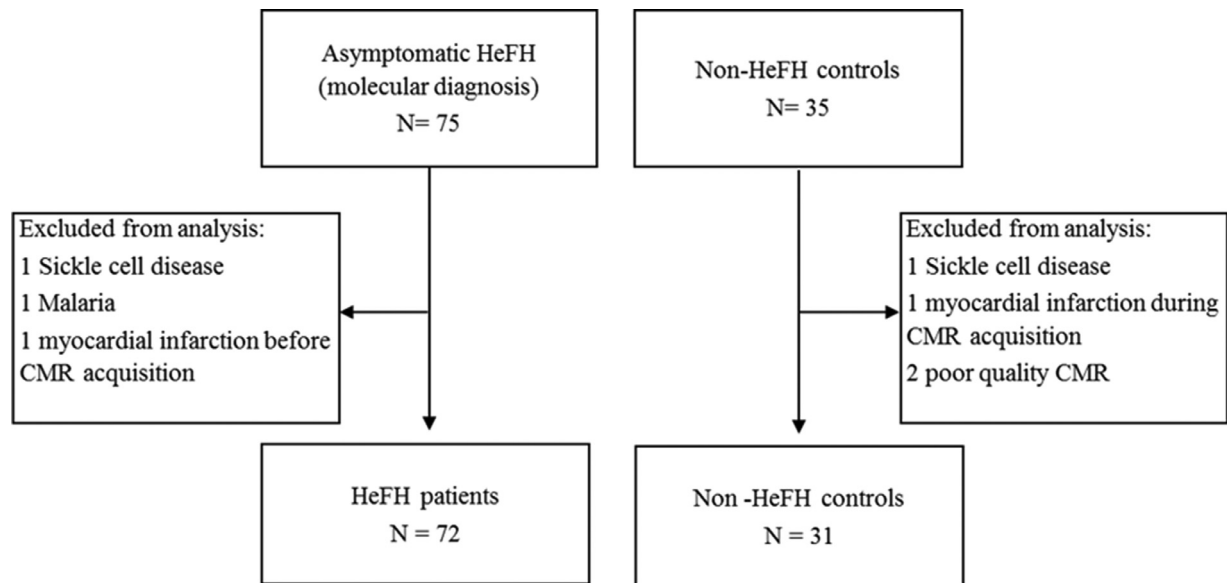


Figure 1. Patients' flowchart. Out of 110 total subjects included in the study, we excluded 7 subjects (3 HeFH and 4 controls) due to the presence of sickle cell disease, malaria, and previous myocardial infarction (not known at the selection visit), DCM or poor quality CMR. CMR, Cardiac Magnetic Resonance; DCM, dilated cardiomyopathy; HeFH, heterozygous familial hypercholesterolemia.

5. Results

5.1. Clinical characteristics

Table 1 summarizes the main clinical and biochemical characteristics of the study population. Cases and controls exhibited comparable demographic and anthropometric features. HeFH subjects had higher pulse pressure ($p=0.001$, Wilcoxon Mann Whitney) and a lower diastolic blood pressure ($p=0.026$, Wilcoxon Mann Whitney) compared to controls. They also showed a higher prevalence of family history for CHD ($p < 0.001$, Fischer Exact), a worse lipid profile ($p < 0.001$, $p=0.005$, $p=0.02$ for LDL-C, HDL-C and triglycerides, respectively, Fischer Exact) and a slightly lower GFR ($p=0.038$, Fischer Exact), compared to controls.

Table 2 summarizes the clinical history of HeFH in the case group. On average, patients had been followed-up for more than 30 years and treated for 26 years: most of them were on a combination therapy of statin + ezetimibe. None of them was treated at inclusion by PCSK9 inhibitors.

5.2. Cardiac morphology and function

Table 3 shows CMR characteristics of the two study groups. Although no differences were found in LV volumes ($p = 0.721$ for end-systolic; $p = 0.115$ for end-diastolic, Student's t-test), mass ($p = 0.638$, Student's t-test) and ejection fraction ($p = 0.212$, Student's t-test) between HeFH patients and controls, there was a significantly higher number of patients with hypokinetic segments in the HeFH group ($p = 0.016$, Fischer Exact). Similar RV measures were also found between the two groups except for RV ejection fraction, which was reduced in HeFH patients ($p = 0.004$, Student's t-test). A smaller maximum left atrial volume was also observed in HeFH patients ($p = 0.026$, Student's t-test), with an overall normal LA ejection fraction in both groups ($p = 0.782$, Wilcoxon Mann Whitney).

5.3. Myocardial tissue characteristics

Only five patients among the HeFH group had focal intramyocardial fibrosis, defined by the presence of LGE ($p = 0.188$, Fischer Exact) versus controls (Figure 2). Among those, only one patient exhibited a subendocardial LGE pattern (Figure 3). While no significant

differences in native T1 ($p = 0.446$), T2 ($p = 0.877$, Wilcoxon Mann Whitney) and ECV ($p = 0.051$, Student's t-test) were found between the two groups, post-contrast T1 was significantly lower and ERM significantly higher in HeFH patients as compared to controls ($p < 0.001$ for both, Student's t-test, Figure 4). Female gender ($p < 0.001$, logistic regression) and the presence of xanthoma ($p = 0.045$, logistic regression) were independent clinical associates of a low post-contrast T1 in the HeFH group (Table 4) in a multivariate model that also included age, BMI, family history, GFR and the presence of CAC.

A composite evaluation criterion was built, resulting from the combination of presence of LGE and/or high native T1 and/or high ERM (defined as \geq mean + 1.5 SD corresponding to thresholds of 1065-88ms and 65-13%, respectively). Fifteen subjects (20.8%) in the HeFH group versus 0 in the control group ($p < 0.000$, Fischer Exact) exhibited some degree of intramyocardial fibrosis according to this criterion and such difference remained significant after adjustment for age, gender, family history of cardiovascular disease, current smoking, metabolic syndrome and pulse pressure. The addition of ECV to the composite criteria did not provide any further discrimination.

5.4. LV CMR measures and cholesterol burden in HeFH

Native and post-contrast T1, ECV and ERM were not associated with an increased cholesterol burden. Subjects with a higher cholesterol burden (defined according to a threshold of 15486 mg/dL-years, representing the median cholesterol burden in the FH group) exhibited a higher LV remodeling index, calculated as the LV mass to volume ratio (0.626 ± 0.12 vs. 0.549 ± 0.08 g/mL in low cholesterol burden, $p = 0.008$, Wilcoxon Mann Whitney). This association remained significant after adjustment for age, gender, BMI and SBP (Table 5).

6. Discussion

This is the first study to characterize myocardial tissue alterations using CMR in asymptomatic high-risk HeFH patients. Our study revealed that LGE was present only in few of these HeFH patients. Besides, while no changes in myocardial native T1, T2 and ECV were found, post-contrast T1 was significantly lower in asymptomatic FH patients, pointing an expansion of the interstitial space. However, a

Table 1
Study population main characteristics.

	Cases(N=72)	Controls(N=31)	p
Demographic and anthropometric data			
Age, years	48.94 ± 5.00	49.94 ± 3.71	0.324
Male sex, n (%)	42 (58.33)	18 (58.06)	0.980
BMI, kg/m ²	25.44 ± 4.29	25.30 ± 3.16	0.863
BSA, m ²	1.854 ± 0.20	1.824 ± 0.16	0.470
Waist-to-Hip Ratio	0.925 ± 0.081	0.928 ± 0.053	0.831
Blood pressure			
SBP mmHg	114.10 ± 11.45	112.13 ± 10.08	0.410
DBP mmHg	68.6 ± 8.9	72.6 ± 9.98	0.026
PP mmHg	45.5 ± 8.6	39.6 ± 6.9	0.001
MAP mmHg	87.36 ± 9.14	88.87 ± 9.41	0.446
Heart Rate, bpm	65.74 ± 10.49	66.77 ± 12.98	0.670
Cardiovascular Risk Factors			
Current Smoking, n (%)	20 (27.78)	9 (29.03)	0.593
Arterial Hypertension, n (%)	12 (16.67)	5 (16.13)	1.000
Metabolic Syndrome ^a , n (%)	18 (25.0)	3 (9.68)	0.109
Family history of early CHD, n (%)	35 (48.61)	1 (3.45)	< 10 ⁻⁴
Lp(a) > 50 mg/dl, n (%)	16 (23.53)	3 (9.68)	0.168
High Cardiovascular Risk ^b , n (%)	69 (95.83)	26 (83.87)	0.051
Medication, n (%)			
ARB, n (%)	7 (9.7)	3 (9.7)	0.050
ACEI, n (%)	1 (1.39)	2 (6.5)	
BB, n (%)	3 (4.2)	0 (0.0)	
CCB, n (%)	7 (9.7)	4 (12.9)	
Diuretic, n (%)	3 (4.2)	1 (3.2)	
Aspirin, n (%)	5 (4.94)	0 (0.0)	0.188
Lipid Profile			
LDL-C, mg/dl	174.89 ± 56.87	117.39 ± 27.31	< 10 ⁻⁴
HDL-C, mg/dl	53.0 ± 15.7	61.9 ± 14.3	0.005
TG, mg/dl	115.08 ± 81.07	87.81 ± 33.57	0.018
Lp(a), mg/dl	19 (9;180)	12.0 (9;117)	0.278
Other Biochemistry			
Fasting glucose, mmol/l	4.98 ± 0.59	4.89 ± 0.58	0.819
Haematocrit, %	42.23 ± 3.14	41.63 ± 2.73	0.361
HbA1c, %	5.67 ± 0.29	5.55 ± 0.34	0.064
Creatinine, μmol/l	77.3 ± 14.8	72.4 ± 13.3	0.110
GFR, ml/min/1.73m ²	86.1 ± 24.7	90.6 ± 14.4	0.038

ACEI, Angiotensin Converting Enzyme Inhibitor; ARB, Angiotensin Receptor Blocker; BB, beta-blocker; BSA, Body Surface Area; CCB, calcium channel blocker; CHD, Coronary Heart Disease; DBP, Diastolic BP; GFR, glomerular filtration rate; HDL-C, HDL-cholesterol; LDL-C, LDL-cholesterol; Lp(a), lipoprotein (a); MAP, Mean Arterial Pressure; PP, Pulse Pressure; SBP, Systolic BP; TG, triglycerides.

^a Metabolic Syndrome was defined according to the following criteria: Waist Circumference ≥ 80cm (women) or 94cm (men) AND ≥ 2 criteria among: TG ≥ 150 mg/dl; HDL-c < 50 mg/dl (women) or 40 mg/dl (men); SBP ≥ 130 or DBP ≥ 85 mmHg (or antihypertensive therapy); Fasting glucose ≥ 5.6 mmol/l (or antidiabetic therapy).

^b High cardiovascular risk was defined according to the presence of at least one of the following: male sex, age ≥ 40; family history of premature CHD; antihypertensive drug; metabolic syndrome; tendon xanthoma; LDL-C ≥ 250 mg/dl; HDL-c < 40 mg/dl; Lp(a) ≥ 50 mg/dL.

Table 2
Clinical characteristics of HeFH patients.

Familial Hypercholesterolemia	N=72
Age at diagnosis, years	17.93 ± 11.7
Duration of disease since diagnosis, years	30.9 ± 11.2
Extravascular lipid deposit, n (%)	
Xanthoma	17 (23.6)
Xanthelasma	2 (2.8)
Corneal arcus	5 (6.9)
Lipid-Lowering Treatment	
Current lipid-lowering therapy, n (%)	61 (84.72)
Previously treated, n (%)	8 (11.1)
Never treated, n (%)	3 (4.17)
Age at initiation of LLT, y	22.8 ± 11.3
Duration of LLT since diagnosis, years	26.9 ± 11.2
Statin, n (%)	
Moderate intensity	18 (64.2)
High intensity	10 (35.7)
Statin + cholestyramine	1 (1.39)
High intensity	1 (100)
Statin + Ezetimibe	30 (41.67)
Moderate intensity	14 (46.7)
High intensity	16 (53.3)
Ezetimibe	1 (1.39)
Fibrate	1 (1.39)
Cholesterol Burden (N=56)	
Total cholesterol at diagnosis, mg/dL-year	753.6 ± 447
Sum of total cholesterol after diagnosis, mg/dL-year	8204.3 ± 3247
Total Cholesterol Burden, mg/dL-year	16058.9 ± 3644
Coronary Burden (N=63)	
CAC score, HU	185.4 ± 371
CAC score > 0, n (%)	44 (69.8)
CAC score > 100, n (%)	23 (36.5)

Total Cholesterol Burden was calculated according to the following formula: [(Age at diagnosis × TC at diagnosis) + Sum of yearly TC since diagnosis]. LLT, Lipid-Lowering Treatment; CAC, coronary artery calcium; HU, Hounsfield Unit.

combined CMR marker of dense and interstitial myocardial fibrosis was found to be more prevalent in HeFH patients, as compared to non-HeFH controls, after adjustment for established CV risk factors. Furthermore, the presence of xanthoma at diagnosis, suggesting a more severe clinical presentation of HeFH, was independently associated with such lower myocardial post-contrast T1. Our results on post-contrast T1 are in line with previous findings from the Multi-

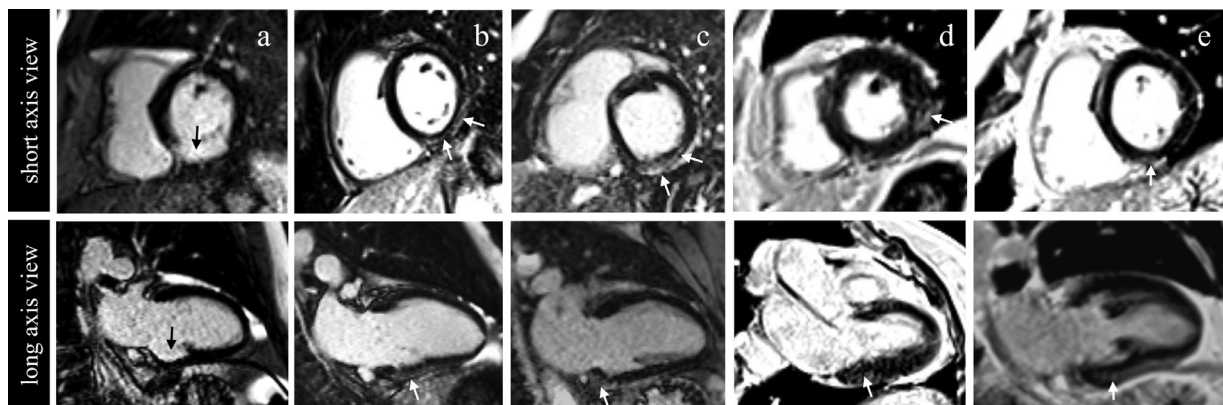


Figure 2. Illustration of late gadolinium enhancement patterns found in 5 patients. Short (top row) and long axis (bottom row) views in magnitude (a,b,c) and phase sensitive (d,e) inversion recovery images. An ischemic pattern was found in patient a with inferior basal infarct (black arrows). Non ischemic patterns (white arrows) included epicardial LGE (patient b,c) and intramural or junctional LGE (patients d,e).

Table 3
Cardiac Magnetic Resonance (CMR) parameters in the study groups.

	Cases(N=72)	Controls(N=31)	p
Left Ventricle			
LV Mass, g	90.17 ± 24.23	88.59 ± 22.90	0.714
LV Mass index ^a , g/m ²	48.15 ± 9.57	47.74 ± 9.65	0.638
LV End-systolic Volume, mL	59.1 ± 16.0	59.8 ± 17.2	0.851
LV End-systolic Volume index ^a , mL/m ²	31.79 ± 7.4	32.39 ± 8.3	0.721
LV End-diastolic Volume, mL	152.2 ± 29.3	158.8 ± 32.5	0.313
LV End-diastolic Volume index ^a , mL/m ²	81.91 ± 11.91	86.27 ± 14.18	0.115
LV Stroke volume, mL	93.1 ± 18.1	98.9 ± 19.8	0.141
LV Ejection fraction, %	61.43 ± 5.8	62.67 ± 5.68	0.212
LV Cardiac Output, L/mn	6.08 ± 5.8	6.59 ± 1.8	0.207
LV Mass-to-Volume, g/ml	0.57 (0.4; 1.1)	0.55 (0.4; 0.8)	0.222
LV longitudinal strain, %	-19.48 ± 2.41	-19.53 ± 2.45	0.920
LV systolic SR, s ⁻¹	-0.904 ± 0.12	-0.889 ± 0.19	0.694
LV early diastole SR, s ⁻¹	0.837 ± 0.16	0.857 ± 0.22	0.940
LV late diastole SR, s ⁻¹	0.389 ± 0.129	0.372 ± 0.20	0.665
Right ventricle			
RV End-systolic Volume, mL	69.1 ± 19.9	63.2 ± 17.9	0.155
RV End-systolic Volume index ^a , mL/m ²	37.08 ± 9.0	34.22 ± 8.2	0.139
RV End-diastolic Volume, mL	159.0 ± 34.7	158.5 ± 34.8	0.951
RV End-diastolic Volume index ^a , mL/m ²	85.44 ± 14.5	86.37 ± 15.22	0.774
RV Stroke volume, mL	89.9 ± 19.6	95.4 ± 19.9	0.198
RV Ejection fraction, %	56.9 ± 5.9	60.5 ± 5.3	0.004
RV Cardiac Output, L/min	5.86 ± 1.4	6.3 ± 1.5	0.144
LV myocardial wall motion			
≥ 1 segment hypokinetic, n (%)	12 (16.67)	0 (0.0)	0.016
≥ 1 segment akinetic, n (%)	1 (1.39)	0 (0.0)	1.000
LV myocardial tissue characterization by CMR			
Presence of LGE, n (%)	5 (6.94)	0 (0.0)	0.188
Pre-contrast T1, ms	1014.14 ± 37.32	1015.4 ± 26.27	0.446
Post-contrast T1, ms	430.62 ± 55.21	476.06 ± 42.99	<10 ⁻⁴
T2, ms	48.22 ± 3.11	48.26 ± 2.85	0.877
Partition coefficient (λ)	0.4218 ± 0.04	0.4351 ± 0.03	0.087
ECV, %	24.36 ± 2.57	25.41 ± 2.17	0.051
ERM, %	57.44 ± 5.99	53.04 ± 4.88	0.001
Left Atrium			
LA Maximum volume, mL	63.33 ± 18.6	68.59 ± 14.7	0.058
LA Maximum volume index ^a , mL/m ²	34.14 ± 9.21	37.55 ± 7.66	0.026
LA Minimum volume, mL	21.49 ± 9.9	23.0 ± 7.1	0.130
LA Minimum volume index ^a , mL/m ²	11.50 ± 4.94	12.49 ± 3.95	0.126
LA ejection fraction, %	67.19 ± 7.65	66.89 ± 5.86	0.782

ECV, Extracellular Volume; ERM, T1 Enhancement Rate in the Myocardium; LA, Left Atrium; LGE, Late Gadolinium Enhancement; LV, Left Ventricle; RV, Right Ventricle; SR, Strain Rate.

^a Mass and volumetric values are indexed for Body Surface Area.

Ethnic Study of Atherosclerosis [23]. In this study which involved 1840 subjects (156 with prior CVD), dyslipidaemia was associated with a decreased post-contrast myocardial T1, without changes in any other CMR parameters. A 10-15ms decrease in post-contrast T1 was associated with an increased risk of cardiovascular events in subjects without previous myocardial focal scar after 10 years follow-up [23]. In patients with heart failure and preserved ejection fraction a significant decrease in post-contrast T1 has been found, associated with worse cardiovascular outcomes [24]. Early diastolic dysfunction has been previously observed in young HeFH patients, together with a thicker LV wall and a higher LV mass [25]. In our long-term followed-up population, with a preserved LV and LA morphology and ejection fraction, this finding was not confirmed, as shown by normal strain and SR values compared to controls, thus suggesting that tissue impairment may depend on cholesterol burden and thus anticipate further organ dysfunction leading to cardiovascular disease.

Animal studies have previously shown a direct relationship between hypercholesterolemia and myocardial lipid accumulation, showing that a chronic exposure to high cholesterol levels is associated with a 3-5 fold increased lipid accumulation in myocardial

tissue, both at the intracellular and interstitial level [26,27]. In humans, lipid accumulation plays an important role in inflammation and ischemia-reperfusion process in subjects after acute myocardial infarction, being responsible for an impaired LV remodeling [28]. Our findings confirm this hypothesis, showing a direct relationship between lifelong cholesterol exposure and LV remodeling, a hallmark of heart failure.

Together with the presence of xanthoma, female sex was associated with a lower post-contrast T1 among HeFH subjects. Interestingly, HeFH women exhibited significantly lower post-contrast T1 values than non-HeFH female controls, in the absence of other LV or RV functional indexes (data not shown).

Native T1 has proven a high sensitivity and accuracy in characterizing myocardial tissue: the presence of oedema or increased interstitial space and diffuse fibrosis are two main determinants of a high native T1, whereas lipid or iron overload are associated with low native T1 [10,29]. In the present study, we did not find any changes in native T1 and no differences in ECV between HeFH and controls. Native T1 values may be pseudo-normalized by a composite signal resulting from concomitant presence of interstitial fibrosis and lipids, but to the best of our knowledge this has not yet been explored. The presence of high ECV, suggesting an excessive deposition in collagen, would have further strengthened the hypothesis of interstitial myocardial fibrosis. However, coherent with the findings on native T1, we did not observe any increase in ECV.

One might note the slightly higher standard deviation of native T1 in HeFH patients as compared to controls revealing a more pronounced interindividual difference in myocardial characteristics in the HeFH population. Higher variability of post contrast T1 vs. pre-contrast T1 has been previously reported. Further analysis using a composite criterion combining presence of LGE with high native T1 and high ERM, which was shown to act as a surrogate of interstitial changes in both myocardium [18] and liver [16,17] confirmed the presence of myocardial structural changes in 20-8% of the HeFH population, against 0 in the control group.

This study has several limitations. First, no causality can be derived from our observations, due both to the observational design of the study and to the insufficient statistical power. Also, this was a monocentric study and cholesterol burden evaluation was not available for the whole study population. Data interpretation cannot be generalized to the whole population as the specificity of the acquisition protocol is limited to one center. The prevalence of concomitant risk factors that can alter T1 and T2 quantification, was comparable between HeFH and non-HeFH subjects. Therefore, the comparison was not made against a healthy population but against subjects with the same common cardiovascular risk factors, namely hypertension and smoke. Results must therefore be interpreted with caution. Indeed, a healthy control group would have allowed to better understand the contribution of the HeFH status and common cardiovascular risk factors on the myocardium tissue changes in this population. This suggests that absolute and generalizable CMR thresholds cannot be derived from the study, and that the differences observed are relative to the HeFH status. The molecular diagnosis of familial hypercholesterolemia was in fact the main distinguishing factor between the two groups, allowing a discrimination of CMR changes related to this condition.

Although we did not find a direct relationship between the presence of subclinical coronary atherosclerosis and myocardial T1 on CMR, we cannot exclude that the presence of CAC, found in more than half the HeFH group, may have an impact on myocardial remodeling. Kidney function may impact the post-contrast T1 finding. However, although a slightly lower GFR was observed in HeFH as compared to controls, GFR was not a significant predictor of low post-contrast T1 beyond xanthoma in this study population.

In conclusion, our findings support the presence of structural changes in the myocardium of HeFH patients that are associated with

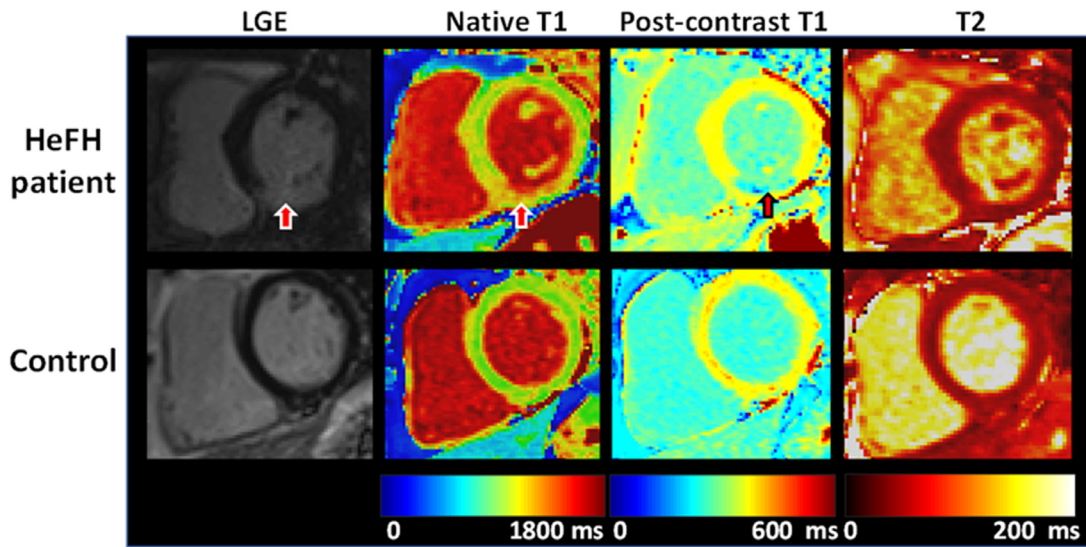


Figure 3. Cardiac Magnetic Resonance changes in a patient with Familial Hypercholesterolemia. This figure shows CMR findings of an asymptomatic HeFH patient with subendocardial myocardial infarction (upper figure) compared to a healthy control (lower figure). Red arrows point at the damaged area, evidenced by LGE and T1 mapping. T1 mapping is a new measure of myocardial fibrosis with CMR, where a parametric reconstructed image of the myocardium is obtained. Each pixel's intensity corresponds to the T1 relaxation time of the corresponding myocardial voxel. Late gadolinium enhancement (LGE): the increase in gadolinium concentration within fibrotic tissue causes T1 shortening, which appears as bright signal intensity in the CMR image. CMR, Cardiac Magnetic Resonance; HeFH, Heterozygous Familial Hypercholesterolemia.

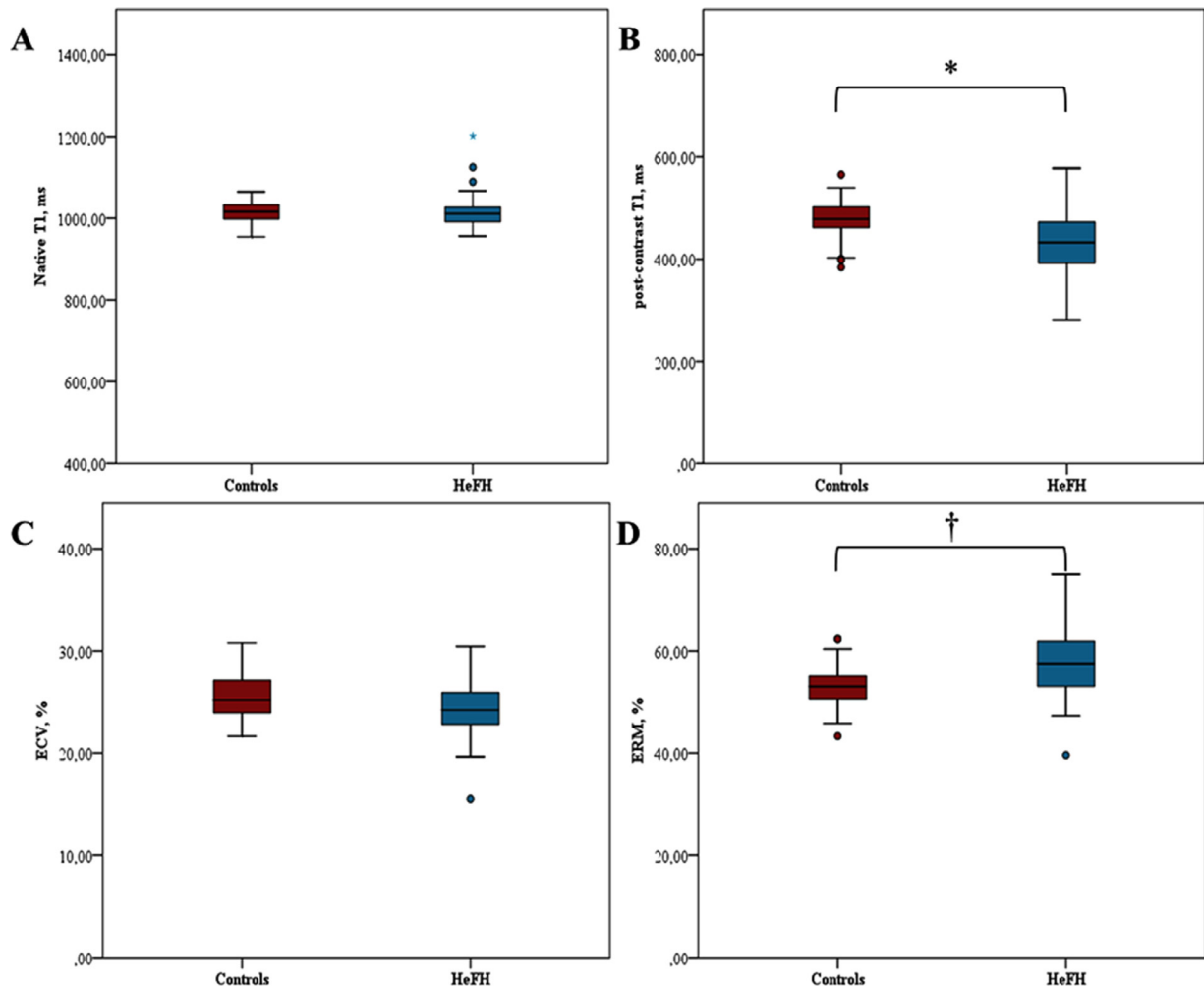


Figure 4. Myocardial tissue characterization in the study population, stratified according to the absence/presence of HeFH. We aimed at comparing T1 mapping markers in HeFH subjects (blue boxplots, N=72) versus age and sex-similar controls (red boxplots, N=31). Only non-infarcted segments were considered for this analysis. We found a similar distribution in native T1 (a) and ECV (c). Patients with HeFH had a lower post-contrast T1 (b) and a higher ERM (d) compared control subjects, pointing an expansion of the interstitial space that suggests interstitial fibrosis. * $p < 0.001$; † $p < 0.005$. Student t-test was performed to compare variables between groups. ECV, extracellular volume; ERM, enhancement rate myocardium. HeFH, heterozygous Familial Hypercholesterolemia.

Table 4
Clinical associates of a low post-contrast T1

	Low post-contrast T1 ^a		
	HR	95 % CI	p
Sex, female	18.186	3.65-90.64	< 0.001
Xanthoma	5.221	1.04-26.28	0.045
Age	0.959	0.83-1.11	0.570
BMI	0.958	0.83-1.11	0.574
Family history	1.304	0.34-4.99	0.699
GFR	1.008	0.967-1.05	0.697
CAC > 0	1.506	0.38-5.96	0.560

BMI, body mass index; CAC, coronary artery calcium; GFR, glomerular filtration rate

^a Model also including LDL-C, Lp(a) and systolic BP.

Table 5
Association of total cholesterol burden with CMR morpho-functional parameters.

	Cholesterol burden, mg/dL-year			
	Univariate		Multivariate ^a	
	β	p	β	p
LV mass, g	0.261	0.052	0.205	0.049
LV Volume, mL	-0.218	0.107	-0.241	0.067
LV Mass to Volume, g/mL	0.520	< 0.001	0.493	< 0.001
LV Ejection Fraction, %	0.135	0.321	0.228	0.137
LV myocardial tissue characterization				
Pre-contrast T1, ms	0.032	0.817	0.141	0.346
Post-contrast T1, ms	0.094	0.492	0.015	0.915
Partition coefficient (λ)	-0.075	0.584	-0.035	0.830
ECV, %	-0.134	0.325	0.037	0.802
ERM, %	-0.081	0.554	0.019	0.888
Presence of LGE, n	0.000	0.117	0.000	0.350

BMI, Body mass index; ECV, extracellular volume; ERM, enhancement rate myocardium; LGE, late gadolinium enhancement; LV, Left Ventricle; SBP, systolic BP.

^a Adjusted for age, gender, BMI and SBP.

Declaration of Competing Interest

AG declares having received honoraria from Akcea Therapeutics, AMGEN, Sanofi and Regeneron, Novartis, MSD; **DR** declares having received honoraria from AMGEN (Research Grant), Sanofi, Novartis, Roche, AMGEN, Daiichi Sankyo, MSD (Fees for lecture/consulting and travel grants); **AC** has received honoraria from Amgen SAS and Alexion Pharma France SAS, and is currently receiving a grant from Alexion Pharma France SAS; **SB** declares having received honoraria from Amgen, Sanofi; **EB** declares having received honoraria from, AstraZeneca, AMGEN, Genfit, MSD, Sanofi and Regeneron, Danone, Aegerion, Lilly, Ionis-pharmaceuticals. **Remaining authors** have nothing to disclose.

Acknowledgments

We are grateful to Amgen SAS and the ICAN Institute of Cardiometabolism and Nutrition for their helpful economic and logistic support.

References

- Nordstgaard BG, Chapman MJ, Humphries SE, Ginsberg HN, Masana L, Descamps OS, et al. Familial hypercholesterolaemia is underdiagnosed and undertreated in the general population: guidance for clinicians to prevent coronary heart disease: consensus statement of the European Atherosclerosis Society. *Eur Heart J* 2013;34:3478–3490a. doi: [10.1093/eurheartj/ehd273](https://doi.org/10.1093/eurheartj/ehd273).
- Watts GF, Gidding SS, Mata P, Pang J, Sullivan DR, Yamashita S, et al. Familial hypercholesterolaemia: evolving knowledge for designing adaptive models of care. *Nat Rev Cardiol* 2020;17:360–77. doi: [10.1038/s41569-019-0325-8](https://doi.org/10.1038/s41569-019-0325-8).
- EAS Familial Hypercholesterolaemia Studies Collaboration (FHSC). Global perspective of familial hypercholesterolaemia: a cross-sectional study from the EAS Familial Hypercholesterolaemia Studies Collaboration (FHSC). *Lancet Lond Engl* 2021 S0140-6736(21)01122-3. doi: [10.1016/S0140-6736\(21\)01122-3](https://doi.org/10.1016/S0140-6736(21)01122-3).
- Gallo A, Giral P, Carrié A, Carreau V, Béliard S, Bittar R, et al. Early coronary calcifications are related to cholesterol burden in heterozygous familial hypercholesterolemia. *J Clin Lipidol* 2017;11:704–11 e2. doi: [10.1016/j.jacl.2017.03.016](https://doi.org/10.1016/j.jacl.2017.03.016).
- Miname MH, Bittencourt MS, Moraes SR, Alves RIM, Silva PRS, Jannes CE, et al. Coronary Artery Calcium and Cardiovascular Events in Patients With Familial Hypercholesterolemia Receiving Standard Lipid-Lowering Therapy. *JACC Cardiovasc Imaging* 2018. doi: [10.1016/j.jcmg.2018.09.019](https://doi.org/10.1016/j.jcmg.2018.09.019).
- Santos RD. Screening and management of familial hypercholesterolemia. *Curr Opin Cardiol* 2019;34:526–30. doi: [10.1097/HCO.0000000000000660](https://doi.org/10.1097/HCO.0000000000000660).
- Stokes KY, Granger DN. The microcirculation: a motor for the systemic inflammatory response and large vessel disease induced by hypercholesterolemia? *J Physiol* 2005;562:647–53. doi: [10.1113/jphysiol.2004.079640](https://doi.org/10.1113/jphysiol.2004.079640).
- Garg P, Underwood SR, Senior R, Greenwood JP, Plein S. Noninvasive cardiac imaging in suspected acute coronary syndrome. *Nat Rev Cardiol* 2016;13:266–75. doi: [10.1038/nrcardio.2016.18](https://doi.org/10.1038/nrcardio.2016.18).
- Mewton N, Liu CY, Croisille P, Bluemke D, Lima JAC. Assessment of myocardial fibrosis with cardiovascular magnetic resonance. *J Am Coll Cardiol* 2011;57:891–903. doi: [10.1016/j.jacc.2010.11.013](https://doi.org/10.1016/j.jacc.2010.11.013).
- Taylor AJ, Salerno M, Dharmakumar R, Mapping Jerosch-Herold MT1. Basic Techniques and Clinical Applications. *JACC Cardiovasc Imaging* 2016;9:67–81. doi: [10.1016/j.jcmg.2015.11.005](https://doi.org/10.1016/j.jcmg.2015.11.005).
- Gallo A, Pérez de Isla L, Charrière S, Vimont A, Alonso R, Muñoz-Grijalvo O, et al. The Added Value of Coronary Calcium Score in Predicting Cardiovascular Events in Familial Hypercholesterolemia. *JACC Cardiovasc Imaging* 2021 S1936-878X (21)00501-5. doi: [10.1016/j.jcmg.2021.06.011](https://doi.org/10.1016/j.jcmg.2021.06.011).
- Pérez de Isla L, Watts GF, Alonso R, Díaz-Díaz JL, Muñoz-Grijalvo O, Zambón D, et al. Lipoprotein(a), LDL-cholesterol, and hypertension: predictors of the need for aortic valve replacement in familial hypercholesterolaemia. *Eur Heart J* 2021. doi: [10.1093/eurheartj/ehaa1066](https://doi.org/10.1093/eurheartj/ehaa1066).
- Gallo A, Charrière S, Vimont A, Chapman MJ, Angoulvant D, Boccara F, et al. SAFE-HEART risk-equation and cholesterol-year-score are powerful predictors of cardiovascular events in French patients with familial hypercholesterolemia. *Atherosclerosis* 2020;306:41–9. doi: [10.1016/j.atherosclerosis.2020.06.011](https://doi.org/10.1016/j.atherosclerosis.2020.06.011).
- D Cerqueira Manuel, J Weissman Neil, Vasken Dilsizian, K Jacobs Alice, Sanjiv Kaul, et al. Standardized Myocardial Segmentation and Nomenclature for Tomographic Imaging of the Heart. *Circulation* 2002;105:539–42. doi: [10.1161/hc0402.102975](https://doi.org/10.1161/hc0402.102975).
- Lamy J, Soulat G, Evin M, Huber A, de Cesare A, Giron A, et al. Scan-rescan reproducibility of ventricular and atrial MRI feature tracking strain. *Comput Biol Med* 2018;92:197–203. doi: [10.1016/j.combiomed.2017.11.015](https://doi.org/10.1016/j.combiomed.2017.11.015).
- Yoon JH, Lee JM, Paek M, Han JK, Choi BI. Quantitative assessment of hepatic function: modified look-locker inversion recovery (MOLL) sequence for T1 mapping on Gd-EOB-DTPA-enhanced liver MR imaging. *Eur Radiol* 2016;26:1775–82. doi: [10.1007/s00330-015-3994-7](https://doi.org/10.1007/s00330-015-3994-7).

the severity of the clinical manifestation and the extent of long-term high-cholesterol exposure. The contribution of the gene-environment interaction in the pathophysiology of myocardial tissue changes in HeFH remains unknown. Further randomized-controlled long-term follow-up studies are needed to confirm the efficacy of a new proposed algorithm that contemplates CMR for HeFH cardiovascular risk stratification.

Contributors

AG, PG, DR, EB, AR, NK contributed to the literature search, conception and design of the research.

AG, AM, AK, AGi, KB, JES, VC, RB, MG, PC, AR, NK contributed to data collection, analysis, and interpretation.

AG and NK drafted the manuscript.

EB, AC, SB, AR critically revised the manuscript.

All authors gave final approval and agreed to be accountable for all aspects of work ensuring integrity and accuracy.

Funding

Amgen, ICAN Institute of Cardiometabolism and Nutrition.

Data sharing statement

Individual unidentified participant data will be made available on reasonable request through email correspondence with the corresponding author after approval of a proposal, with a signed data access agreement.

- [17] Besa C, Bane O, Jajamovich G, Marchione J, Taouli B. 3D T1 relaxometry pre and post gadoteric acid injection for the assessment of liver cirrhosis and liver function. *Magn Reson Imaging* 2015;33:1075–82. doi: [10.1016/j.mri.2015.06.013](https://doi.org/10.1016/j.mri.2015.06.013).
- [18] Huber AT, Lamy J, Bravetti M, Bouazizi K, Bacoyannis T, Roux C, et al. Comparison of MR T1 and T2 mapping parameters to characterize myocardial and skeletal muscle involvement in systemic idiopathic inflammatory myopathy (IIM). *Eur Radiol* 2019;29:5139–47. doi: [10.1007/s00330-019-06054-6](https://doi.org/10.1007/s00330-019-06054-6).
- [19] Agatston AS, Janowitz WR, Hildner FJ, Zusmer NR, Viamonte M, Detrano R. Quantification of coronary artery calcium using ultrafast computed tomography. *J Am Coll Cardiol* 1990;15:827–32.
- [20] Bruckert E, Kalmykova O, Bittar R, Carreau V, Béliard S, Saheb S, et al. Long-term outcome in 53 patients with homozygous familial hypercholesterolaemia in a single centre in France. *Atherosclerosis* 2017;257:130–7. doi: [10.1016/j.atherosclerosis.2017.01.015](https://doi.org/10.1016/j.atherosclerosis.2017.01.015).
- [21] Sacré K, Brihaye B, Hyafil F, Serfaty J-M, Escoubet B, Zennaro M-C, et al. Asymptomatic myocardial ischemic disease in antiphospholipid syndrome: a controlled cardiac magnetic resonance imaging study. *Arthritis Rheum* 2010;62:2093–100. doi: [10.1002/art.27488](https://doi.org/10.1002/art.27488).
- [22] Kwong RY, Sattar H, Wu H, Vorobiof G, Gandla V, Steel K, et al. Incidence and prognostic implication of unrecognized myocardial scar characterized by cardiac magnetic resonance in diabetic patients without clinical evidence of myocardial infarction. *Circulation* 2008;118:1011–20. doi: [10.1161/CIRCULATIONAHA.107.727826](https://doi.org/10.1161/CIRCULATIONAHA.107.727826).
- [23] Ambale-Venkatesh B, Liu C-Y, Liu Y-C, Donekal S, Ohyama Y, Sharma RK, et al. Association of myocardial fibrosis and cardiovascular events: the multi-ethnic study of atherosclerosis. *Eur Heart J Cardiovasc Imaging* 2019;20:168–76. doi: [10.1093/ehjci/jey140](https://doi.org/10.1093/ehjci/jey140).
- [24] Marzluft BA, Bonderman D, Tufaro C, Pfaffenberger S, Graf A, Hülsmann M, et al. Diffuse myocardial fibrosis by post-contrast T1-time predicts outcome in heart failure with preserved ejection fraction. *J Cardiovasc Magn Reson* 2013;15:M6. doi: [10.1186/1532-429X-15-S1-M6](https://doi.org/10.1186/1532-429X-15-S1-M6).
- [25] Di Salvo G, D'Aiello AF, Castaldi B, Fadel B, Limongelli G, D'Andrea A, et al. Early left ventricular abnormalities in children with heterozygous familial hypercholesterolemia. *J Am Soc Echocardiogr Off Publ Am Soc Echocardiogr* 2012;25:1075–82. doi: [10.1016/j.echo.2012.07.002](https://doi.org/10.1016/j.echo.2012.07.002).
- [26] Vilahur G, Casani L, Juan-Babot O, Guerra JM, Badimon L. Infiltrated cardiac lipids impair myofibroblast-induced healing of the myocardial scar post-myocardial infarction. *Atherosclerosis* 2012;224:368–76. doi: [10.1016/j.atherosclerosis.2012.07.003](https://doi.org/10.1016/j.atherosclerosis.2012.07.003).
- [27] Osipov RM, Bianchi C, Feng J, Clements RT, Liu Y, Robich MP, et al. Effect of hypercholesterolemia on myocardial necrosis and apoptosis in the setting of ischemia-reperfusion. *Circulation* 2009;120:S22–30. doi: [10.1161/CIRCULATIONAHA.108.842724](https://doi.org/10.1161/CIRCULATIONAHA.108.842724).
- [28] Cohn JN, Ferrari R, Sharpe N. Cardiac remodeling—concepts and clinical implications: a consensus paper from an international forum on cardiac remodeling. Behalf of an International Forum on Cardiac Remodeling *J Am Coll Cardiol* 2000;35:569–82. doi: [10.1016/s0735-1097\(99\)00630-0](https://doi.org/10.1016/s0735-1097(99)00630-0).
- [29] Haaf P, Garg P, Messroghli DR, Broadbent DA, Greenwood JP, Plein S. Cardiac T1 Mapping and Extracellular Volume (ECV) in clinical practice: a comprehensive review. *J Cardiovasc Magn Reson* 2016;18:89. doi: [10.1186/s12968-016-0308-4](https://doi.org/10.1186/s12968-016-0308-4).